Received: 14 March 2023 | Revised: 14 May 2023 | Accepted: 23 May 2023
DOI: 10.22034/ecc.2023.397277.1645
Journal of Medicinal and Pharmaceutical Chemistry Research
SAMI

FULL PAPER

Microwave-assisted hydrothermal synthesis as a nanocomposite with superior adsorption capacity for efficient removal of toxic Maxillon blue(GRL) dye from aqueous solutions

Rana S. Al-Shemary[a] |Aseel M. Aljeboree[b,*] |Ayad F. Alkaim[b]

[a]*Department of Pharmaceutical Chemistry, College of Pharmacy, University of Babylon, Babylon, Iraq*

[b]*Department of Chemistry, College of Sciences for Women, University of Babylon, Hillah, Iraq*

In this study, a microwave assisted hydrothermal technique was employed for the synthesis of CNT/ZnO nanocomposite. Carbon nanotubes were obtained from incineration stacks in furnaces. They were treated with concentrated (0.1 N) H_3PO_4. The structures of nano-composites were characterized *via* utilizing powder (FE-SEM), and (TEM). Specific surface area (BET), total pore volume, and mean pore size were too studied through utilizing Bruneuer Emmatt Teller (BET) technique to refer to the properties surface of the nano-composites. Several operational factors like initial concentration of GRL dye, amount of CNT/ZnO nanocomposite, solution of pH, and temperature solution by utilize of CNT/ZnO nanocomposite in the adsorption of GRL dye. It was found that removal percentage E % rises with increase weight of the nanocomposite until all the active sites of the nanocomposite are saturated. The percentage removal of GRL dye rises from 45.42% to 90.853% for solution pH increase about 3.2-10.5. The result of the kinetic was studied by means of several model kinetic like first model, the second model, and Elcovich model was found to be the maximum kinetic model second-order (R^2=0.9986) for our adsorption investigation. The thermodynamic factor having change Gibbs energy (ΔG), change entropy (ΔS), and change enthalpy (ΔH). The negative value of ΔH (-9.043 kJ.mol^{-1}) was estimated for the adsorption method and the adsorption is a physical and exothermic, positive value ΔS (13.8469 J.mol^{-1} K^{-1}), and the values negative of (ΔG) in the range temperature of 10-30 ^{o}C, confirming that the dye adsorption on to Nano composite was spontaneous.

***Corresponding Author:**
Aseel M. Aljeboree
E-mail: annenayad@gmail.com
Tel.: +964 780 2426 078

KEYWORDS

Dye; adsorption; kinetic; thermodynamic; exothermic; CNT; zinc oxide.

Introduction

In recent years, the aquatic environment has been polluted with human pollutants like heavy metals, dyes, pesticides, organic and inorganic pollutants, and others. Organic dyes are commonly found in wastewater produced by industries such as textiles, paper, leather, pharmaceuticals, printing, etc.[1-8]. Maxillon blue dye is a basic dye that causes many health problems such as skin and eye irritation, diarrhea, shortness of breath, cough, and nausea. Therefore, the treatment

of industrial wastewater loaded with these dyes is a major concern for the researcher. Therefore, several techniques have been used such as membrane separation, adsorption, photocatalysis, advanced oxidation process, ozone, and others. Among these technologies, adsorption is preferred for the treatment of industrial wastewater loaded with dyes [9-11]. This technique makes the absorbent materials highly efficient. The most important of these surfaces is carbon nanotube, which has a good internal porous interface and a high surface area. It is considered as one of the better and utmost usually utilized absorbent material in water treatment. Zinc oxide is characterized by its environmentally friendly nature and is widely used in the photocatalytic process, but there are few studies on its use in the adsorption method. In this research, ZnO was loaded on to CNT to make the surface with high efficiency in relation to removal dyes.

Adsorption experiments

Preparation of CNT decorated (zinc oxide /nanocomposite)

Carbon nanotubes were obtained from incineration stacks in furnaces, they were treated with concentrated (0.1 N) H_3PO_4 with continuous stirring for two hours, and then washed by distilled water in several times, filtered and dried at (65 °C). Zinc oxide nanoparticles were prepared in the laboratory by taking 5 g of oxalic acid, and 5 g of zinc acetate dissolved in distilled water and mixing for 30 minute, and then addition 0.1 g of CNT to it and mixing it well in ultrasound for 30 minute. Before preparing the mixture, it was placed in a hydrothermal solution at 160 °C for about 24 h, and the surface was washed different times by distilled water and dry at 60 °C for 12 h to obtain the powder used in the experiment.

Batch adsorption

Stock solution of Maxillon blue (GRL) dye 500 mg/L was prepared via dissolving 0.5 g dye in 500 mL of distilled water. A 0.05 g ZnO/CNT nanocomposite in 100 mL a suitable concentration of dye was shaken in shaker at 130 rpm at 20 °C. After removal of the nanocomposite filtration by centrifuge of 3000 rpm, the GRL concentrations in the supernatant were estimation via a UV-Vis spectrophotometer. The (E%) and (Qe, mg/g) were estimated by Equations 1 and 2.

$$Removal\ persentage\ \% = \frac{\mathrm{Co}-\mathrm{Ce}}{\mathrm{Co}} * 100 \qquad (1)$$

$$adsorption\ capacity = (\mathrm{Co} - \mathrm{Ce})/m * V \qquad (2)$$

Where, Co primary concentration of GRL and Ce equilibrium concentration of GRL in the solution (mg/L), V volume (mL) of GRL, and m is the quantity of nanocomposite (g).

Results and discussion

Characterization of CNT/ZnO nanocomposites

The surface area and structure pore of CNT/ZnO nanocomposite are estimated using the nitrogen adsorption isothermal system. The nitrogen isotherms adsorption-desorption and distributions pore size of CNT/ZnO nanocomposite is represented. The isotherm profile of CNT/ZnO demonstrates a small hysteresis loop that can be categorized as kind IV. The surface area, total pore volume, and average pore diameter were improved after the incorporation of carbone on to the grafted ZnO as shown in Figure 1. The interfacial interactions among carbone and ZnO have a great impact on the pore structure of material as evident from this study [12-17].

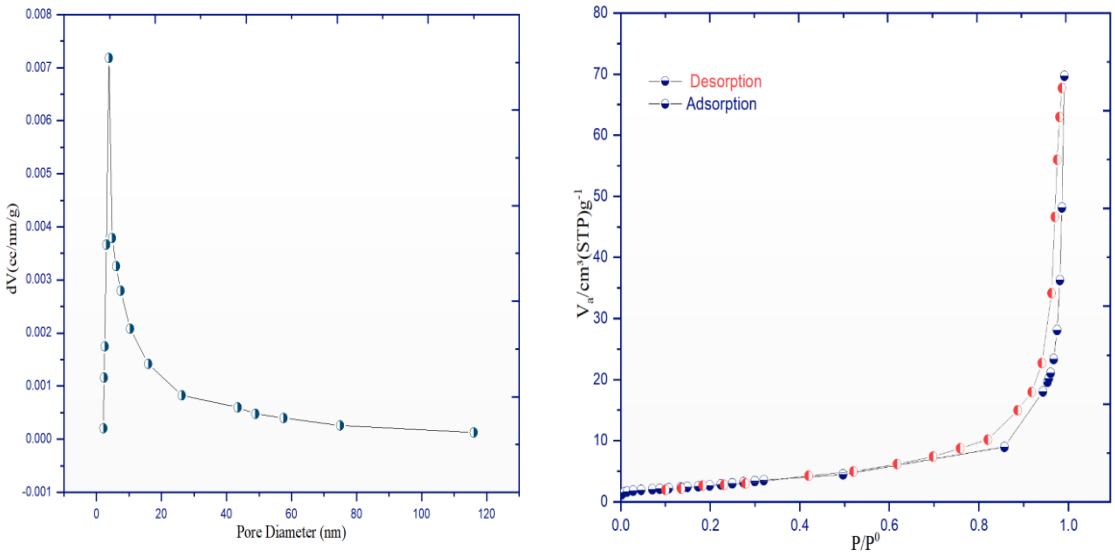

FIGURE 1 Surface area and structure pore of CNT/ZnO nanocomposite

The FE-SEM method was utilized to clarify the morphology of the prepared CNT/ZnO nanocomposite. Figure 2a shows an image of carbon nanotubes, where the appearance of clusters similar to tubes spread on the nanotubes surface, and through Figure 2b, zinc oxide was loaded on nanotubes carbon. We notice the spread of zinc on the surface in the form of small spherical clusters, but after the adsorption process. The emergence of many irregular spherical assemblies and the surface CNT/ZnO nanocomposite became more swollen clear evidence of the GRL loading inside the surface and occurrence of the adsorption method, as appeared in Figure 2c.

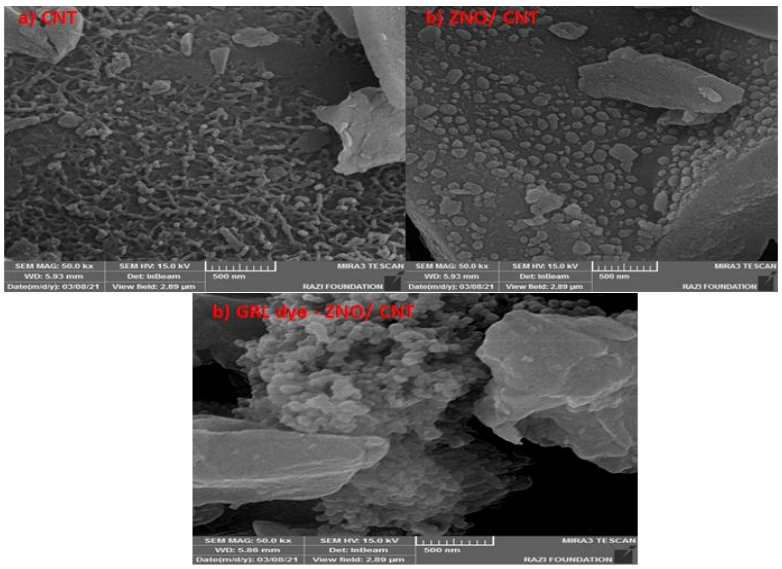

FIGURE 2 FESEM of (a) CNT, (b) CNT/ZnO nanocomposite, and (c) CNT/ZnO nanocomposite loading GRL dye

The TEM technique was utilized to estimate the characteristics of prepared surface before and after adsorption, as it was observed that some dark spots seemed on the surface, evidence of loading GRL on the prepared surface and the occurrence of adsorption method [18], as depicted in Figure 3.

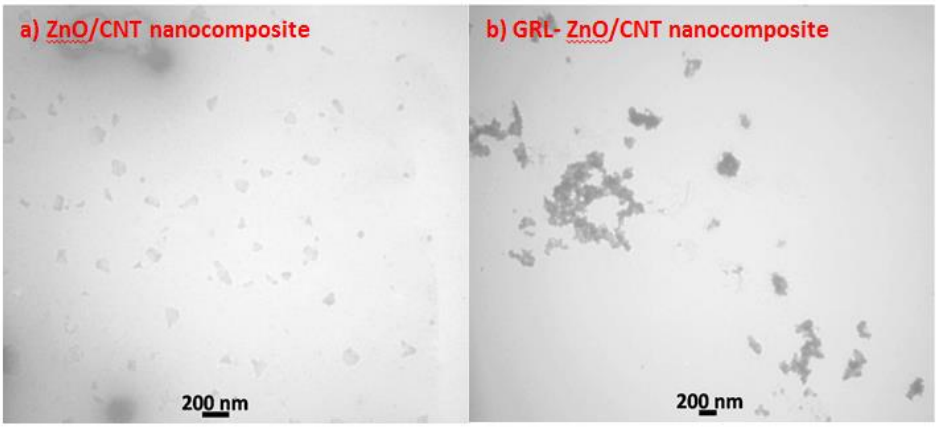

FIGURE 3 TEM of (a) ZnO/CNT and (b) GRL-ZnO/CNT nanocomposite

Effect of different parameter

Effect of weight of nanocomposite

The quantity of nanocomposite utilized in adsorption is for the most part because it limits the equilibrium sorbent-sorbate in the way and can too be utilized to predict the treatment cost of adsorbent per unit of solution GRL [19]. The influence of mass adsorbent on E% of GRL was studied and the results are demonstrated in Figure 4. The percentage removal E% of dye rise through rise in mass adsorbent. For instance, E% of dye at equilibrium increased about 15.14%-97.82% when the mass adsorbent increased about 0.003-0.15 g. The increased percentage% of GRL via nanocomposite was as a data of raised surface area and increased adsorption site occasioned through greater than before mass adsorbent. Similar data have been previously reported [20-22]. Furthermore, above 0.1 g, there is hardly any improvement in removal capacity of dye.

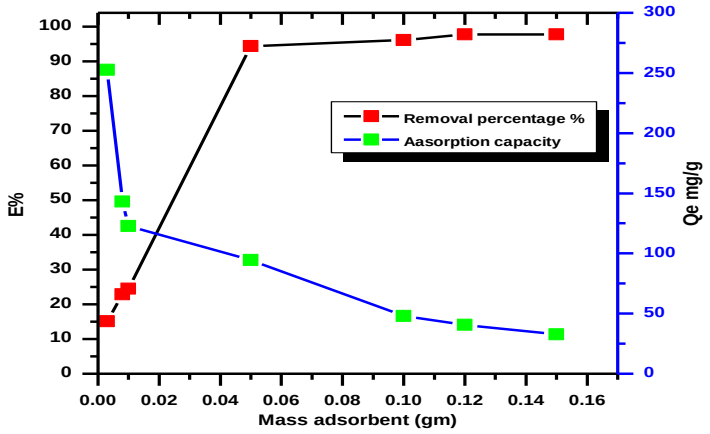

FIGURE 4 Effect of mass of nanocomposite on the E% and quantity of adsorbed dye

Effect of solution pH

One of the utmost important parameter that affects the adsorption behavior of nanocomposite is the solution pH. The adsorption of dye on to nanocomposite as a function of pH was studied for pH values rang about 3.2-10.5 by a primary concentration CRL of 100 $mg.L^{-1}$ (Figure 5).

The percentage removal of GRL dye a rises from 90.42%- 95.853% for a solution pH increase about 3.2 to 6.8. Therefore, it is clear from the result that the adsorption process is the dependent pH, the adsorption capacity

and the removal E% of GRL adsorbed increasing through solution pH and being at best at pH 6.8. Several reasons may be attributed to the adsorption of GRL dye via the nanocomposite relative to pH [23-25].

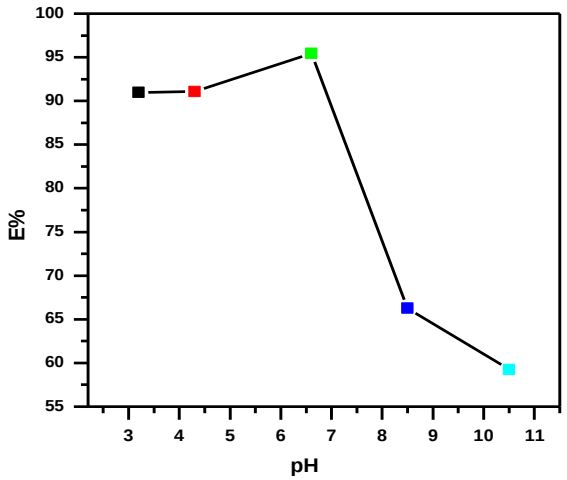

FIGURE 5 Effect of pH on the removal E% onto nanocomposite (Exp. Condition: adsorbent dosage 0.05 g, Temperature = 25 °C, and equilibrium time 60 min)

Effect of solution temperature and thermodynamic parameter

To observe the influence of solution temperature, the adsorption studies were carried out for the concentration of GRL 100 mg L^{-1} at different temperatures 10, 20, and 30 ^{o}C, at pH 6.6.

Figure 6 illustrates the adsorption efficiency against the adsorption time at different temperatures. It was observed that equilibrium adsorption of GRL raised from 58.1 -239.5 mg g^{-1} by temperature solution rise 10 to 30 ^{o}C, indicating the nature ex-othermic of the reaction adsorption. To study the adsorption thermo-dynamics of GRL on nanocomposite, basic three thermos-dynamic factor, (ΔH), (ΔS), and (ΔG) were estimated using equations [18,26].

$$\text{Ln Ka} = \frac{\Delta S}{R} - \frac{\Delta H}{RT} \quad (3)$$

$$K_a = \frac{Ce}{qe} \quad (4)$$

$$\Delta G = -RT \text{ Ln } K_a \quad (5)$$

Where, T temperature solution (K), K_a adsorption equilibrium constant, and R gas constant. (Change enthalpy) and (change entropy) were estimated from the slope and intercept from the plot of ln(Xm) vs. 1000/T(K) (figure not shown).

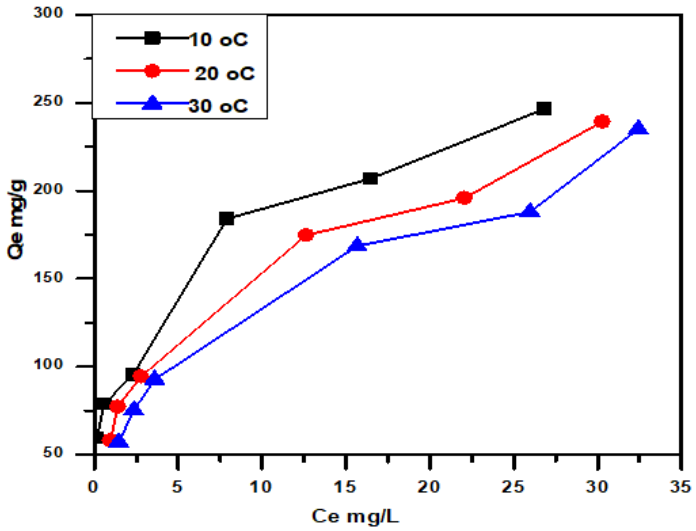

FIGURE 6 Adsorption at several temperature of GRL dye onto CNT/ZnO

The value of (ΔG) was estimated using Equation 5. The result is presented in Table 1. The negative value of ΔH (-9.043 kJ.mol^{-1}) indicates that adsorption of GRL on to nanocomposite is an exothermic. The negative values of (ΔG) in the range temperature of 10-30 ^{o}C, confirming that the adsorption of GRL on to Nano composite was spontaneous and favorable thermodynamically. The positive value ΔS (13.8469 J mol^{-1} K^{-1}) indicates a decrease in the degree of freedom of adsorption GRL on to ZnO/ CNT [27,28].

TABLE 1 Thermo-dynamic parameter of Adsorption for GRL onto surface

ΔH (KJ.mol^{-1})	ΔG (kJ.mol^{-1})	ΔS (J.mol-1.K^{-1})
-9.04313	-19.212989 -19.891893 -20.570797	13.8469

Adsorption kinetics

Equilibrium time is another key factor affect the impurity uptake via the sorbent. The influence of agitation duration and the GRL dye (10-100 mgL^{-1}) on the dye uptake was carefully studied at 20 ^{o}C. Figure 7 illustrates the improvement efficiency by time and primary conc. The uptake rate is initially fast until an value equilibrium constant at 1 h [29]. The rapid uptake rate at the first sorption was caused via the utmost the reactive groups and avail-ability of the outer surface of the sorbent.

It is evident that the adsorption efficiency (qe) rises from 83.71 to 231.84 mg/g as the GRL concentration is greater about 10-100 mg/L. Because greater primary concentration leads to larger mass transfer driving force, thus leading to higher dye sorption, we fixed the equilibrium time to 1 h for our batch investigational [30] .

Adsorption kinetic result was analyzed using the kinetic adsorption Lagergren first model calculated by Equation 6.

$$Ln(q_e-q_t)= Lnq_e-K_1t \quad (6)$$

Where, K_1 (min^{-1}) is the first-model constant rate adsorption and time t (min). Values of K_1 and equilibrium adsorption density q_e at 20 ^{o}C were determine from the plots of ln(q_e–q_t) vs. t for several primary

concentration of GRL (Figure 7). The kinetic second-order can be expressed as Equation 7:

$$\frac{1}{q_t} = \frac{1}{K^2 q_e^2} + \frac{1}{q_e} \text{ t} \qquad (7)$$

The nonlinear model of the Chemisorption (Elovich kinetic model) [30] was calculated by Equation 8.

$$q_t = \frac{1}{\beta} 1\beta \ln(\alpha\beta) + \frac{1}{\beta} \ln t \qquad (8)$$

Intercept of the linear plot of t/q_t vs. t, as appeared in Figure 5.

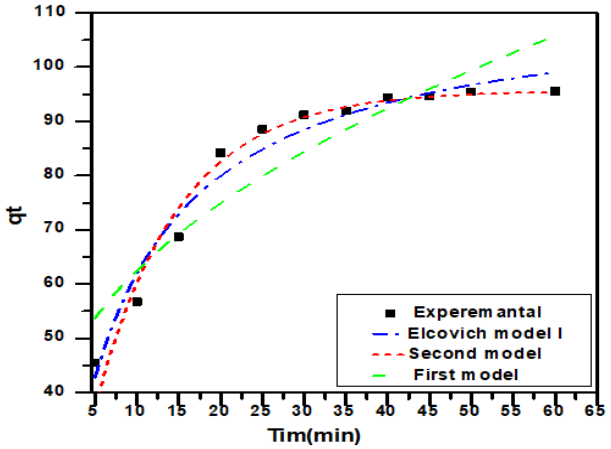

FIGURE 7 Adsorption isotherm three kinetic adsorption first, second, and Elcovich models

TABLE 2 Adsorption kinetic Factors of GRL on CNT/ZnO

Kind	Factors	Value	*R2*
First model	q_e (mg g^{-1})	33.323	0.565
	k_f (min^{-1})	0.055	
Second model	q_e (mg g^{-1})	95.45	0.9986
	k_s (gmg^{-1} min^{-1})	0.0610	
Elovich model	α (mg g^{-1} min^{-1})	111.13	0.921
	β (g min^{-1})	1.422	

The kinetic model data for the first-order, the second-order kinetic, and Elcovch models adsorption appear in Table 2. The nonlinear plots of q_t vs. time (kinetic adsorption second-order) indicated the best agreement among the investigational and estimation values q_e for several primary concentrations of GRL. Likewise, the correlation coefficients of the kinetic second model (R^2 > 0.9986) were greater than kinetic first model. It can be said that the adsorption second kinetic model better than the First model [31,32].

Conclusion

Through the results that were reached, after the process of loading zinc oxide onto multi carbon nanotube, the surface became highly efficient and the surface area increased. A low-cost, environmentally friendly surface with a very high capacity in removing industrial dyes. With an increase weight of nanocomposite, the removal percentage E% increases, as the percentage of removal reach (95%) at the weight of (0.05 g) and any

increase in weight did not notice any significant increase because of saturation of most active sites of the surface. The percentage removal of GRL dye a rises from 90.42%-95.853% for a solution pH increase about 3.2 to 6.8. The percentage removal increases with increasing temperature and the best result at 25 °C, Gibbs energy (ΔG) the values negative in the range temperature of 10-30 °C, confirming that GRL adsorption on to nanocomposite was spontaneous and the positive value (ΔS 13.8469 $J.mol^{-1}$ K^{-1}).

Acknowledgements

The financial support for this research was provided by Ministry of Higher Education Malaysia under FRGS Grant no. 2019-0147-103-02.

Conflict of Interest

The authors declare that there is no conflict of interest.

Orcid:

Rana S. Al-Shemary:
https://orcid.org/0000-0001-7657-4543
Aseel M. Aljeboree:
https://orcid.org/0000-0001-5397-3330
Ayad F. Alkaim:
https://orcid.org/0000-0003-3459-4583

References

[1] G. Moussavi, A. Alahabadi, K. Yaghmaeian, M. Eskandari, Preparation, characterization and adsorption potential of the NH4Cl-induced activated carbon for the removal of amoxicillin antibiotic from water, *Chem. Eng. J.*, **2020**, *217*, 119-128. [crossref], [Google Scholar], [Publisher]

[2] Y. Liu, Y.Chen, Y. Shi, D. Wan, J. Chen, S. Xiao, Adsorption of toxic dye Eosin Y from aqueous solution by clay/carbon composite derived from spent bleaching earth, *Water Environ. Res.*, **2021**, *93*, 159-169. [crossref], [Google Scholar], [Publisher]

[3] A.M. Aljeboree, A.N. Alshirifi, Spectrophotometric determination of phenylephrine hydrochloride drug in the existence of 4-aminoantipyrine: Statistical study, *Int. J. Pharm. Res.*, **2018**, *10*, 576-584. [crossref], [Google Scholar], [Publisher]

[4] M.N. Masood, N. Mohammed, K.S. Husien, Characterization of eight natural dyes as synthesizer for dye-sensitized solar cells technology, *J. Med. Chem. Sci.*, **2023**, *6*, 693-701. [crossref], [Google Scholar], [Publisher]

[5] O. Ajani, K. Bello, A. Kogo, Synthesis and characterization of acid dyes based on substituted pyridone using metal complexes (1:2) and study of their application on nylon fbrics (6.6), *Appl. Organomet. Chem.*, **2023**, *3*, 61-72. [crossref], [Google Scholar], [Publisher]

[6] F.A. Hiawi, I.H. Ali, Study the adsorption behavior of food colorant dye indigo carmine and loratadine drug in aqueous solution, *Chem. Methodol.*, **2022**, *6*, 720-730. [crossref], [Google Scholar], [Publisher]

[7] Z.A. Messaoudi, D. Lahcene, T. Benaissa, M. Messaoudi, B. Zahraoui, M. Belhachemi, A. Choukchou-Braham, Adsorption and photocatalytic degradation of crystal violet dye under sunlight irradiation using natural and modified clays by zinc oxide, *Chem. Methodol.*, **2022**, *6*, 661-676. [crossref], [Google Scholar], [Publisher]

[8] W. Al-Graiti, S.M. Merdas, Evaluation of some eco-friendly food residues for removal of methylene blue dye from aqueous solutions, *J. Med. Chem. Sci.*, **2023**, *6*, 1044-1054. [crossref], [Pdf], [Publisher]

[9] A.M. Aljeboree, A.N. Alshirifi, A.F. Alkaim, Removal of pharmaceutical amoxicillin drug by using (Cnt) decorated clay/ fe2 o3 micro/nanocomposite as effective adsorbent: Process optimization for ultrasound-assisted adsorption, *Int. J. Pharm. Res.*, **2019**, *11*, 80-86. [crossref], [Google Scholar], [Publisher]

[10] M.B. Alqaragully, H.Y. AL-Gubury, A.M. Aljeboree, F.F. Karam, A.F. Alkaim, Monoethanolamine: Production plant, *Rese. J. Pharm. Biol. Chem. Sci.*, **2015**, *6*, 1287-1296. [Google Scholar], [Publisher]

[11] S. Thakur, J. Chaudhary, A. Thakur, O. Gunduz, W.F. Alsanie, C. Makatsoris, V.K. Thakur, Highly efficient poly (acrylic acid-co-aniline) grafted itaconic acid hydrogel: Application in water retention and adsorption of rhodamine B dye for a

sustainable environment, *Chemosphere*, **2022**, *303*, 134917. [crossref], [Google Scholar], [Publisher]
[12] A. Chowdhury, S. Kumari, A.A. Khan, M.R. Chandra, S. Hussain, Activated carbon loaded with Ni-Co-S nanoparticle for superior adsorption capacity of antibiotics and dye from wastewater: kinetics and isotherms, *Colloids Surf. A. Physicochem. Eng. Asp.*, **2021**, *611*, 125868. [crossref], [Google Scholar], [Publisher]
[13] V.O. Njoku, K.Y. Foo, M. Asif, B.H. Hameed, Preparation of activated carbons from rambutan (Nephelium lappaceum) peel by microwave-induced KOH activation for acid yellow 17 dye adsorption, *Chem. Eng. J.*, **2014**, *250*, 198-204. [crossref], [Google Scholar], [Publisher]
[14] A.M. Osman, A.H. Hendi, T.A. Saleh, Simultaneous adsorption of dye and toxic metal ions using an interfacially polymerized silica/polyamide nanocomposite: Kinetic and thermodynamic studies, *J. Mol. Liq.,* **2020**, *314*, 113640. [crossref], [Google Scholar], [Publisher]
[15] U. Kamran, Y.J. Heo, J.W. Lee, S.J. Park, Chemically modified activated carbon decorated with MnO2 nanocomposites for improving lithium adsorption and recovery from aqueous media, *J. Alloys Compd.*, **2019**, *794*, 425-434. [crossref], [Google Scholar], [Publisher]
[16] F. Ansari, M. Ghaedi, M. Taghdiri, A. Asfaram, Application of ZnO nanorods loaded on activated carbon for ultrasonic assisted dyes removal: experimental design and derivative spectrophotometry method, *Ultrason Sonochem*, **2016**, *33*, 197-209.[crossref], [Google Scholar], [Publisher]
[17] W. Jiang, L. Zhang, X. Guo, M. Yang, Y. Lu, Y. Wang, Y. Zheng, G. Wei, Adsorption of cationic dye from water using an iron oxide/activated carbon magnetic composites prepared from sugarcane bagasse by microwave method, *Environ. technol.*, **2021**, *42*, 337-350. [crossref], [Google Scholar], [Publisher]
[18] A.M. Aljeboree, A.B. Mahdi, Synthesis highly active surface of ZnO/AC nanocomposite for removal of pollutants from aqueous solutions: thermodynamic and kinetic study, *Appl. Nanosci.*, **2021**, 1-14. [crossref], [Google Scholar], [Publisher]
[19] B. Gao, H. Yu, J. Wen, H. Zeng, T. Liang, F. Zuo, C. Cheng, Super-adsorbent poly (acrylic acid)/laponite hydrogel with ultrahigh mechanical property for adsorption of methylene blue, *J. Environ. Chem. Eng.*, **2021**, *9*, 106346. [crossref], [Google Scholar], [Publisher]
[20] A.M. Aljeboree, A.F. Alkaim, Comparative removal of three textile dyes from aqueous solutions by adsorption: As a model (Corn-Cob source waste) of plants role in environmental enhancement, *Plant Arch.*, **2019**, *19*, 1613-1620. [Google Scholar], [Publisher]
[21] A.F. Alkaim, A. Aljobree, White marble as an alternative surface for removal of toxic dyes (Methylene Blue) from aqueous solutions, *Internat. J. Adv. Sci. Technol.*, **2020**, *29*, 5470-5479. [Google Scholar], [Publisher]
[22] Z.A.A. Alradaa, Z.M. Kadam, June. Preparation, Characterization and Prevention Biological pollution of 4 (4-Benzophenylazo) Pyrogallol and their Metal Complexes, *IOP Conf Ser Earth Environ Sci*, 2021, *790*, 012038, IOP Publishing. [crossref], [Google Scholar], [Publisher]
[23] A.T. Bader, Zaied-A-Mosaa, A.M. Aljeboree, A.F. Alkaim, Removal of Methyl Violet (MV) from aqueous solutions by adsorption using activated carbon from pine husks (plant waste sources), *Plant Arch.*, **2019**, *19*, 898-901. [Google Scholar], [Publisher]
[24] P. Ilgin, H. Ozay, O. Ozay, Selective adsorption of cationic dyes from colored noxious effluent using a novel N-tert-butylmaleamic acid based hydrogels, *React Funct. Polym.*, **2019**, *142*, 189-198. [crossref], [Google Scholar], [Publisher]
[25] S. Pashaei-Fakhri, S.J. Peighambardoust, R. Foroutan, N. Arsalani, B. Ramavandi, Crystal violet dye sorption over acrylamide/graphene oxide bonded sodium alginate nanocomposite hydrogel, *Chemosphere*, **2021**, *270*, 129419. [crossref], [Google Scholar], [Publisher]
[26] S.H.H. Wared, N.D. Radia, Synthesis and characterization of sodium alginate-g-polyacrylic acid hydrogel and its application for crystal violet dye adsorption, *Int. J. Drug Deliv. Technol.*, **2021**, *11*,556-565. [Google Scholar], [Publisher]

[27] W. Konicki, D. Sibera, E. Mijowska, Z. Lendzion-Bieluń, U. Narkiewicz, Equilibrium and kinetic studies on acid dye Acid Red 88 adsorption by magnetic $ZnFe_2O_4$ spinel ferrite nanoparticles, *J. Colloid Interface Sci.*, **2013**, *398*, 152-160. [crossref], [Google Scholar], [Publisher]
[28] S. Thakur, Synthesis, characterization and adsorption studies of an acrylic acid-grafted sodium alginate-based TiO2 hydrogel nanocomposite, *Adsorp. Sci. Technol.*, **2018**, *36*, 458–477. [crossref], [Google Scholar], [Publisher]
[29] M. Ghaedi, B. Sadeghian, A.A. Pebdani, R. Sahraei, A. Daneshfar, C. Duran, Kinetics, thermodynamics and equilibrium evaluation of direct yellow 12 removal by adsorption onto silver nanoparticles loaded activated carbon, *Chem. Eng. J.*, **2012**, *187*, 133-141. [crossref], [Google Scholar], [Publisher]
[30] J.L. Acero, F.J. Benitez, F.J. Real, G. Roldan, Kinetics of aqueous chlorination of some pharmaceuticals and their elimination from water matrices, *Water Res.*, **2010**, *44*, 4158-4170. [crossref], [Google Scholar], [Publisher]
[31] Z.I. Al-Mashhadani, A,M. Aljeboree, N.D. Radia, O.K. Alkadir, Antibiotics removal by adsorption onto eco-friendly surface: characterization and kinetic study, *Int. J. Pharm. Qual. Assur.*, **2021**, *12*, 252-255. [crossref], [Google Scholar], [Publisher]
[32] N.D. Radia, S.M. Kamona, H. Jasem, R.R. Abass, S.E. Izzat, M.S. Ali, S.T. Ghafel, A.M. Aljeboree, Role of hydrogel and study of its high-efficiency to removal streptomycin drug from aqueous solutions. [crossref], [Google Scholar], [Publisher]

How to cite this article: Rana S. Al-Shemary*, Aseel M. Aljeboree, Ayad F. Alkaim. Microwave-assisted hydrothermal synthesis as a Nanocomposite with superior adsorption capacity for efficient removal of toxic Maxillon blue(GRL) dye from aqueous solutions. *Journal of Medicinal and Pharmaceutical Chemistry Research*, 2023, 5(9), 832-841.